

PRODUCTION OF RADIOACTIVITY BY PARTICLE ACCELERATORS

Peter J. Gollon

September, 1975

I. INTRODUCTION

At all accelerators with energies greater than some tens of MeV, induced radioactivity results whenever beams interact with accelerator or beam transport components. Typically these interactions occur at such spots as injection and extraction points and beam splitting stations. Losses at these points are not desirable, and great efforts are often required to reduce them. Beam losses also occur at collimators, scrapers, target areas and beam dumps; these losses are deliberate and cannot be reduced. Consequently, these are usually the most radioactive areas in the accelerator laboratory, and work near them is the largest source of radiation exposures at all laboratories. It is therefore necessary to be able to anticipate the magnitude of the problems involved in such work.

While these loss points are common to all accelerators, the magnitude of the resulting problems depends on many factors unique to each accelerator: The type of particle accelerated, the particle energy, and the geometry and composition of the items being struck. I shall deal with these considerations in turn. What follows is only a general introduction for those not actively involved in this area. The literature should be consulted for details.¹

II. MECHANISMS OF ACTIVATION.

A. Proton Accelerators.

The extranuclear hadron cascade process which has been discussed in previous lectures is the process which produces the major fraction of the induced radioactivity at proton accelerators. Each high energy particle which interacts with a nucleus may be absorbed and/or may knock some nuclei out of the struck nucleus. Additional high energy particles may also be created in the collision. If the resulting nucleus is highly excited, it will de-excite by "boiling off" evaporation neutrons. The entire nuclear reaction process is known as "spallation". Each such reaction is called a "star" because of the many secondary particles radiating from it.

The resulting nucleus may be stable or radioactive. The probability, or cross section, of producing a particular nuclide depends on the target nucleus and on the energy of the incident particle. These cross sections are best determined from experimental data; if such data is lacking, an empirical formula of Rudstam gives a good approximation to cross sections which vary over several orders of magnitude.²

The particles in the cascade continue to propagate and decay or interact until their energy drops below the threshold for nuclear reactions; this is usually between 10 and 50 MeV. However, for some nuclides, neutron capture is an exoergic reaction which can occur at all energies and has a large cross section for thermal neutrons. (The radioactivation of concrete occurs principally by thermal neutron capture on ^{23}Na to produce 15-hour ^{24}Na .)

The excellent book by Barbier contains information on many cross sections which are relevant to radioactivation and describes how to calculate induced activity levels from such data. I will discuss some details of these calculations later. First I would like to discuss some simple rules of thumb which can be used for most "back of the envelope" calculations.

Rule 1: The dose rate \dot{D} (R/hr) at a distance r (meters) from a "point source" of gamma rays is given in terms of the source strength S (Curies) and the photon energy E_γ (MeV), by³

$$\dot{D} = k_\gamma \frac{S}{r^2} \approx \frac{\sum E_\gamma}{2.2} \frac{S}{r^2} \quad (1)$$

Rule 2: In many common materials, about 10% of the nuclear interactions produce a radionuclide with a lifetime longer than a few minutes.

Using these rules, we can for instance calculate the dose rate near a target a tenth of an interaction length long. (If it were much longer, we would have to make a large correction for secondary interactions in the target.) Assume a beam of 10^{11} protons/sec has struck the target for several months - long enough for many of the radionuclides produced to reach their saturation levels. Of the 10^{11} protons/second incident, one tenth interact and a tenth of the interactions yield radionuclides of interest. The resulting decay rate is 10^9 /sec, or $10^9/3.7 \times 10^{10} = 27$ mCi. (1 Curie $\equiv 3.7 \times 10^{10}$ disintegrations/second.) Assuming each decay produces a 1 MeV photon, the dose rate half a meter away is

$$\dot{D} = \frac{1 \text{ Mev} \cdot 0.027 \text{ Ci}}{2.2 \cdot (0.5\text{m})^2} = 0.049 \text{ R/hr} = 49 \text{ mR/hr}$$

-3-

This activity will decay with time in a way which this simple model cannot predict.

Another useful rule relates the total number of stars produced by a single proton in the entire cascade to the incident proton (or hadron) energy:

Rule 3: In a cascade, a proton produces four stars for each GeV of kinetic energy.⁴

Thus a beam of 10^{12} 400 GeV protons/sec (= 0.16 μ A, or 64 kW) produces a total of $4 \times 400 \times 10^{12} = 16 \times 10^{14}$ stars/sec in its beam dump. If 10% of the stars yield a radionuclide of any importance, then the total amount of radioactivity in the dump is

$$\frac{(0.1 \text{ dis/star}) (16 \times 10^{14} \text{ stars/sec})}{3.7 \times 10^{10} \text{ dis sec}^{-1} \text{ Ci}^{-1}} = 4 \text{ kCi.}$$

B. Electron Accelerators

The electron-photon shower, the process whereby high energy electrons interact in bulk matter, is conceptually similar to the hadron shower just described. The principal differences lie in the type of particles which propagate, and in the interactions which produce them. When the initiating electron or photon has an energy greater than several GeV, the predominant interactions are:⁵

1. Bremsstrahlung, in which an e^\pm radiates a photon in the electric field of a nucleus;
2. Pair Production, in which a photon turns into an electron-positron pair in the field of a nucleus.

At lower energies - some tens to a hundred MeV, depending on the material - the following processes for reducing the electron or photon energies become important:

3. Electron-Electron Collisions (ionization), in which an incident electron elastically scatters from an atomic electron, resulting in two lower energy electrons;
4. Compton Scattering, in which photons elastically scatter from atomic electrons, transferring some of their energy to the electrons.

The longitudinal development of the shower is characterized by a quantity known as the "radiation length", X_0 . It is the

distance which the average energy of an electron or photon is reduced by a factor of e . Since the bremsstrahlung and pair production cross sections are proportional to Z^2 , X_0 is approximately proportional to Z^{-2} . Radiation lengths for common materials range from 35 cm for light elements to 6.5 cm for lead.

The number of electrons and photons in the shower increases exponentially with depth (as e^{x/X_0}), with additional electrons and photons being produced by pair production and bremsstrahlung. This continues until the average particle energy is below the "critical energy" for that material; at this point ionization and Compton scattering play a dominant role in removing energy from the shower, and particle multiplication ceases. Because of random variations in each interaction, the cascade dies off only slowly when the mean particle energy reaches the critical energy. The electron shower is therefore characterized by a rapid exponential rise to a maximum, followed by a slower fall.

The shower consists of equal numbers of positrons, electrons, and photons, but only the photons play a significant role in producing nuclear reactions. Most significant are the (γ, n) , $(\gamma, 2n)$, (γ, p) , (γ, pn) and (γ, α) photonuclear reactions.

In a shower initiated by an electron of energy E_0 , the number of photons with energies between E and $E+dE$ is

$$dN(E) \propto \frac{E_0}{E} dE \quad (2)$$

The total track length $g(E)$ is the total distance travelled by all photons in the shower which have energies between E and $E+dE$. It is given by⁶

$$g(E) dE = 0.57 \frac{E_0}{E} X_0 dE \quad (\text{gm/cm}^2) \quad (3)$$

The track length is multiplied by the number of target nuclei per grams and by the reaction cross section to obtain the number of photonuclear reactions initiated by photons of energy E . We then integrate over all possible photon energies to obtain the number of photonuclear reactions in the cascade (the "giant resonance yield"):⁷

$$Y = 0.57 \frac{E_0 X_0 N_0}{A} \int_0^{E_0} \frac{\sigma(E)}{E^2} dE \quad (4)$$

Two factors combine to allow an approximation to the integral. First, the photonuclear cross sections are dominated by the "giant resonance" phenomenon which occurs between 20 and 50 MeV; other processes occur less frequently. In addition,

the photon spectrum is a sharply falling function of energy. The denominator (E^2) may be taken to be equal to its value (E_m^2) at the cross section maximum, and moved outside the integral:

$$Y = 0.57 \frac{E_o X_o N_o}{A E_m^2} \int_0^{E_o} \sigma(E) dE \quad (5)$$

Barbier presents curves of integrated cross sections as a function of target mass for the five photonuclear reactions of interest. His most useful curves are those in which he has combined all the factors in eq. 5 except for the incident electron energy. These are reproduced as fig. 1. To find the number of reactions produced in a shower due to an incident electron of energy E_o , one multiplies the giant resonance yield (read from the appropriate graph) by E_o .

As an example, we calculate the total activity created in an iron target (assumed to be 100% ^{56}Fe) by a 1 μA , 20 GeV electron beam (20 kW of power). The most significant reaction is $^{56}\text{Fe}(\gamma, \text{pn})^{54}\text{Mn}$. The yield for this reaction is 3×10^{-6} per MeV. The incident beam is

$$\frac{10^{-6} \text{ Coul/sec} \times 2 \times 10^4 \text{ MeV}}{1.6 \times 10^{-19} \text{ Coul}} = 1.25 \times 10^{17} \text{ MeV/sec}$$

The reaction rate is then

$$Y = 1.25 \times 10^{17} \text{ MeV/sec} \times 3 \times 10^{-6} / \text{MeV} = 3.8 \times 10^{11} \text{ sec}^{-1}$$

When the 300-day half life ^{54}Mn has been saturated, this will be a total activity of 10 Ci. This is about 1/10 of the activity produced in an iron dump by a proton beam of the same power.

C. Relation between hadron and electron showers.

While hadron and electron showers were just discussed separately, they are in fact connected. In hadron-initiated interactions, about one third of the pions produced are uncharged. These promptly decay into two high-energy photons, which start electron showers. At 400 GeV, about half of the incident proton beam energy is dissipated in the form of electron showers. However, electron showers are much less effective than hadron showers, per MeV of energy, at producing radioactivity, so that this effect may be ignored in hadron cascades.

Conversely, the photonuclear reactions which occur in electron showers liberate nucleons from the struck nuclei. However, since most of these reactions occur near 50 MeV, the escaping nucleons do not have much energy. They are therefore not likely to interact further except by neutron capture, and whether this yields a significant amount of radioactivity depends on the specific materials involved.

III. CALCULATIONAL TECHNIQUES; COMPARISON WITH EXPERIMENT.

In order to provide more accurate, and thus more useful information concerning dose rates due to activation, we must have more or less detailed information concerning the cascade source term, nuclear reaction data, and radiological data. By these terms I mean:

cascade source term: information concerning the spatial distribution and spectra of the particles in the hadron or electron shower which produces the radioactivation of the object of interest ("target").

nuclear reaction data: reaction cross sections for various nuclei in the "target" being transformed into other, radioactive nuclei by the particles in the cascade.

radiological data: nuclear lifetimes, decay schemes, transport of β 's and γ 's out of the activated object (i.e., self-shielding) and flux-to-dose conversion factors.

There are several calculational approaches. Alsmiller and co-workers at Oak Ridge use the most involved technique: they Monte Carlo the cascades, including the intra-nuclear details of each reaction, and then carefully calculate the transport of the decay γ -rays out of the material.⁸ An example of the results obtained from such a calculation is shown in fig. 2.

A different approach is used by Barbier¹. He separates the problem into two parts: the user is given the task of determining the flux of activating particles (hadrons or photons), while Barbier provides information on residual dose rate for a unit activating flux. Barbier derives his cross section data from an empirical formula of Rudstam² (in the case of spallation reactions), or from his own smooth fits to measured photonuclear cross sections. Experimental values of nuclear lifetimes and decay characteristics are entered into the calculations. Transport of β and γ rays out of the material and conversion to dose rate is done in an approximate analytic way. The results may be presented in terms of what Barbier calls the "danger parameter". This is the dose rate in a cavity inside an infinite volume of

-7-

radioactive substance of uniformly distributed activity produced by unit flux (1 particle/cm² sec). Curves of danger parameters for different materials are shown in fig. 3, which are similar to conventional cooling curves. The danger parameter is a function of irradiation and cooling time because isotopes with different lifetimes will saturate and decay differently with time.

We can use one of these curves to determine the dose rate in a real situation involving a thick source by using the following relation:

$$\dot{D} = \frac{\Omega}{4\pi} \cdot \phi \cdot d$$

The dose rate at any point (\dot{D}) is obtained by multiplying the danger parameter (d) by the fractional solid angle the source subtends when seen from the point of interest (Ω), and by the activating flux (ϕ) at the surface of the object.⁹ (The activity several γ absorption lengths into the body does not contribute much to the external dose rate because of self-shielding by the activated object.)

It is possible to obtain the hadron flux at the surface of the object from a Monte-Carlo calculation run for that purpose, or from a collection of "standard" cases.¹⁰ If this is done, one must be careful because many Monte Carlo programs have a low-energy cutoff, below which they cease to follow particles. Since this cutoff may be higher than the thresholds of many activation reactions, use of the "flux" predicted by the Monte Carlo calculation will give an erroneously low value for the activation. Correction for this effect may be made if the ratio of the true flux to the "Monte Carlo flux" is known. This ratio is material-dependent, and to the extent that the spectrum has not reached an equilibrium shape, it is position dependent as well.

Rearranging the factors:

$$\begin{aligned} \dot{D}(t_i, t_c) &= \sum_{\mu} A_{\mu} \{ \exp(-t_c/\tau_{\mu}) - \exp(-[t_i+t_c]/\tau_{\mu}) \} \\ &= \dot{D}(\infty, t_i+t_c) \end{aligned}$$

Thus the dose rate sought is the difference between the dose rates for the case of an infinite irradiation time and two hypothetical cooling times: one equal to the actual irradiation time, the other equal to the actual irradiation plus cooling times.

-8-

It is far easier to make predictions of induced radioactivity than it is to verify those predictions, thus experimental data is hard to come by. Figure 4 shows measurements and calculations made by Barbier and Cooper at CERN.¹¹ The average difference between prediction and measurement is about a factor of two. Other comparisons show similar agreement. When known cross sections and thin targets are used, the agreement is even better.¹²

IV. APPLICATIONS

Life is not really as simple as one might believe from what I have said up until now. First, calculations by different authors disagree with each other, often by factors of two. Second, real life sometimes does not reproduce any author's calculation. (Fortunately, things seem to cool off faster in real life than they do in calculations.) Figure 5 shows a calculation from Oak Ridge, with a number of measured curves added. The curve labelled "accel" is based on the measured cooling of the average dose rate around our 6-km main ring. Our accelerator has been operating for 3 years with essentially constant losses, thus the curve ought to be comparable to the one labelled "one year"; but it falls about a factor of 3 below it for long cooling times.

The curve labelled "neutrino" represents the decay of an area near the target of our dichromatic (narrow band) neutrino target train after a run of 8 months. The beam intensity varied by a factor of about two over this period. Again, the components cool much faster than one would predict.

Finally, the curve marked "AGS" represents the dose rate near the AGS slow external beam splitter.¹³ This unit has been operating for many years, and its decay agrees reasonably well with the predictions for long irradiations. The most obvious explanation for the disagreement of observations and calculations is that possibly a lot more short-lived activity than is expected (or a lot less long-lived activity) is actually being produced. I have no data to substantiate or refute this conjecture, however.

As can be seen from the various graphs of the danger parameter, different materials vary widely in their relative hazards due to activation. Aluminum is preferred to iron because of its lesser activation - the only major long-lived activity produced from aluminum is ^{22}Na . For shielding purposes, CaCO_3 - marble - is excellent for the same reason; in this case the cross section for ^{22}Na production from calcium is even lower. Elements above calcium, however, are capable of readily producing long-lived activity.¹⁴

Sodium, on the other hand, is notorious for causing problems because of its high thermal neutron capture cross sections,

producing ^{24}Na . The effects of even small amounts of sodium in concrete have been studied extensively both theoretically and experimentally.¹⁵ Briefly, concrete containing one percent of sodium by weight produces enough ^{24}Na activity to approximately double the radiation level in the machine enclosure the first day after machine turn-off. Since the major source of sodium in concrete is the aggregate, a proper choice of aggregate, such as limestone, can eliminate this problem.

Another subject which has been studied at some length is the question of radioactivation of air in target and accelerator enclosures.¹⁶ It has been our experience, and that of others, that because of the short half-lives involved (20 min ^{11}C , is the longest) there is no internal exposure hazard. There is an external exposure hazard, but that is smaller than, and no different from the hazard due to radioactivated accelerator components in the same area.

Both proton and electron accelerators produce radioactivity in water when their respective showers cross water cooling paths in beam dumps. Both types of machines are capable of producing many kilocuries of short-lived activity. The SLAC accelerator has a water beam dump, and in fact produces such large activities.¹⁷ Proton accelerators, on the other hand, have less beam power, and their dumps have only small water channels. As a result, our water activity problems are much less severe.

Under normal circumstances, the radioactivation of the water which cools targets and beam dumps presents several distinct problems. The first is gamma exposure from short-lived radionuclides in the water as it passes through pipes and heat exchangers. At SLAC there are dose rates of many R/hour near such items; the corresponding levels at Fermilab are tens of mR/hour. The second problem is the deposition of ^7Be in the deionizing columns needed to maintain the water resistivity. These deionizers will also collect radioactive corrosion products from piping and targets. Besides being sources of external exposure, the activity in these columns must be disposed of in an appropriately safe way. The third problem is that the build-up of large quantities of tritium in the water presents a possible hazard in case of water leaks. These hazards may be minimized and confined by having separate, small volume cooling systems for target systems and beam dumps, by insisting on high quality piping, etc., and by periodically draining the water from the cooling loops for disposal under controlled circumstances.

Where earth is used for hadron shielding it will become activated. This may present difficulties if it is later planned

to excavate the area for additional construction. In addition, the radio nuclides created in the soil may migrate to other areas, and perhaps contaminate surface or underground waters. The most significant nuclides in this regard are ^3H , ^{22}Na and ^{45}Ca . This has been studied experimentally and theoretically at CERN and FERMILAB.¹⁸

Our experience has been that soil activation may be a problem only around the most radioactive target areas. My own rule of thumb is that soil activation need be considered as a possible source of groundwater contamination only for those objects which are so radioactive that they cannot be easily serviced by hand. Since this problem is of limited applicability, I will not dwell on it here; the literature should be consulted for further details.

REFERENCES

1. M. Barbier, Induced Radioactivity, North Holland (1969). This is a comprehensive treatise and contains references to other works not cited below.
2. R. G. Rudstam, Z. Naturforsch. 21a 7 (1966).
3. More exact values of k_{γ} may be found in ref. 1, Appendix A; values of a proportional quantity may be found in Radiological Health Handbook p. 131, U. S. Dept. of H.E.W. (1970).
4. This is true for stars produced by particles above a 15 MeV cutoff in iron. There are about half as many stars produced by particles above a 100 MeV cutoff. R. T. Santoro and T. A. Gabriel, ORNL-TM-3335 (1971).
5. R. B. Leighton, Principles of Modern Physics, P. 690, McGraw-Hill (1959).
6. B. Rossi, High Energy Particles, p. 271, Prentice Hall (1952).
7. Ref. 1, p. 217.
8. See, for example, T. W. Armstrong, et al., Nucl. Sci. Eng. 49, 82 (1973); T. W. Armstrong and R. G. Alsmiller, Jr., ORNL-TM-2498 (1969).
9. Ref. 1, p. 77.
10. A. Van Ginneken and M. Awschalom, High Energy Particle Interactions in Large Targets, Fermilab (1975).
11. M. Barbier and A. Cooper, CERN 65-34 (1965).
12. K. S. Toth, et al., Nucl. Inst. and Meth., 42, 128 (1965).
13. R. Casey, private communication.
14. Ref. 1, p. 37.
15. D. Nachtigall and S. Charalambus, CERN 66-28 (1966); W. S. Gilbert, et al., UCRL-19368 (1969); P. J. Gollon, et al., NAL-TM-250 (1970); T. W. Armstrong and J. Barish, ORNL-TM-2630 (1969).
16. M. Höfert, Proc. Sec. Int'l. Conf. on Accel. Dosimetry and Experience, p. 111, Conf-691101 (1969); K. Goebel in CERN 71-21, p. 3 (1971).

17. G. W. Warren, et al., Proc. Sec. Int'l. Conf. on Accel. Dosimetry and Experience, p. 99, Conf-691101 (1969).
18. F. E. Hoyer, CERN 68-42; and T. Borak, et al., Health Physics 23, p. 679 (1972).

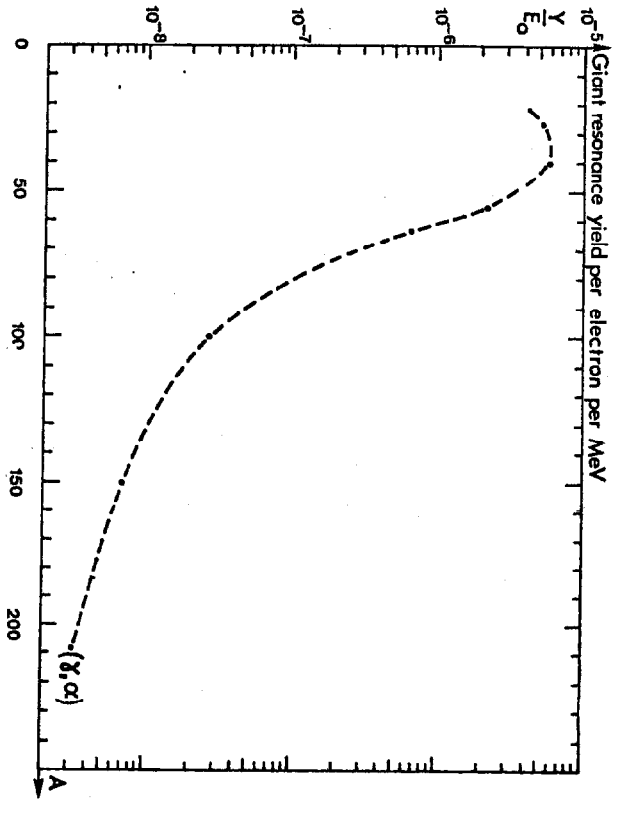
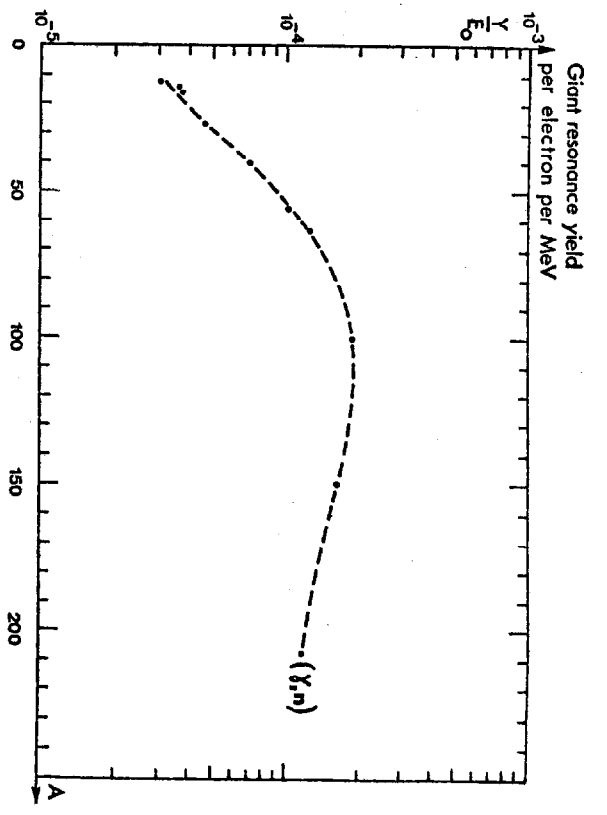
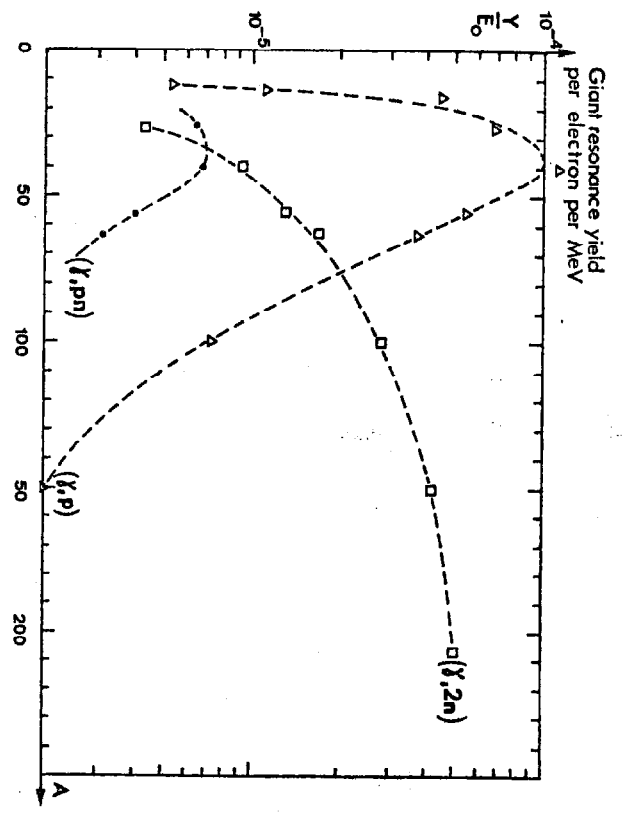


Fig. 1 Giant resonance yield per electron per MeV of energy for fine photo nuclear reactions. (From Ref. 1.)

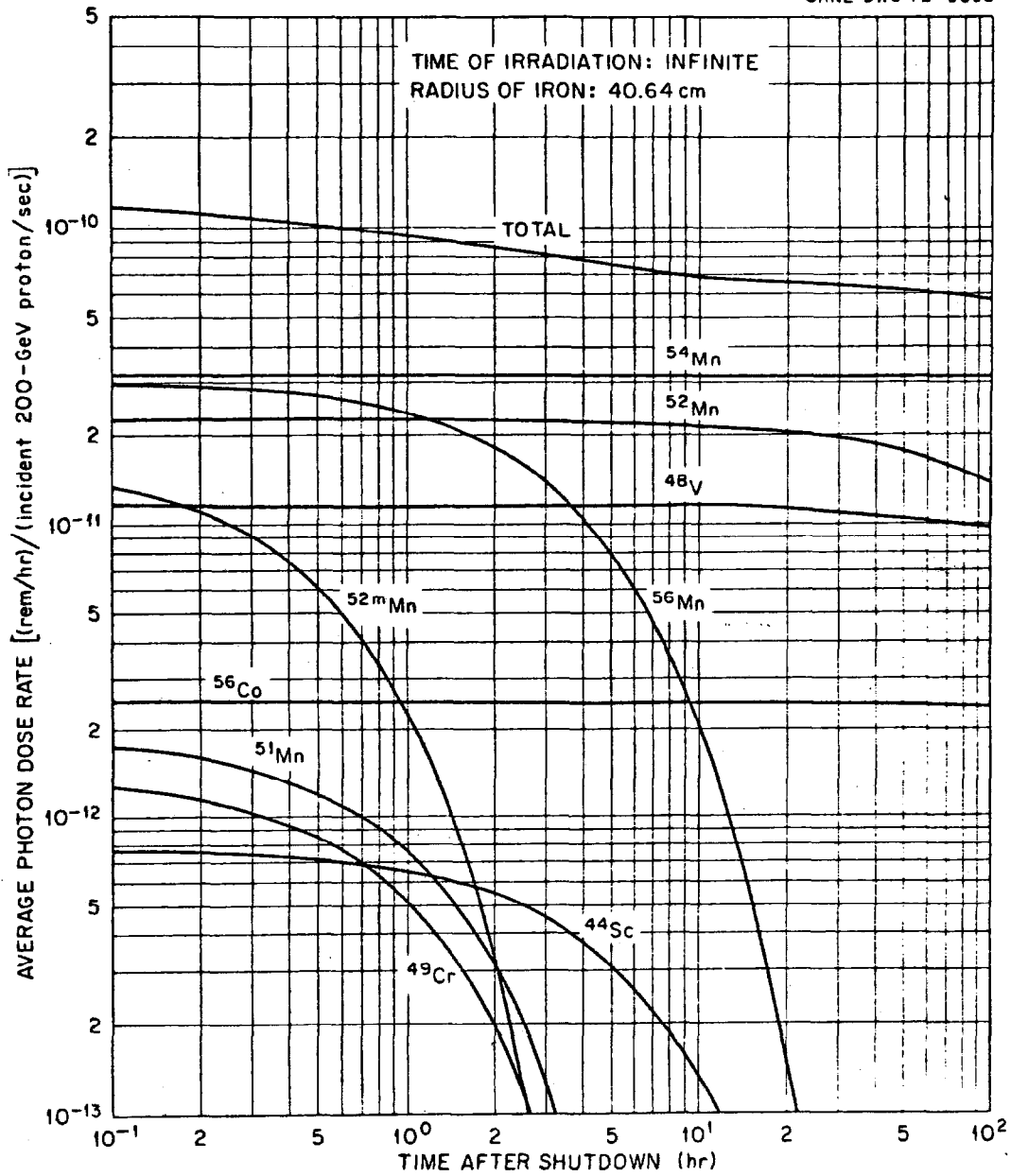


Fig. 2 Contribution of various radionuclides to the total photon dose rate outside a 40.6 cm radius iron beam stop after an infinite irradiation by 200 GeV protons. From T. A. Gabriel and R. T. Santoro, ORNL-TM-3945 (1972).

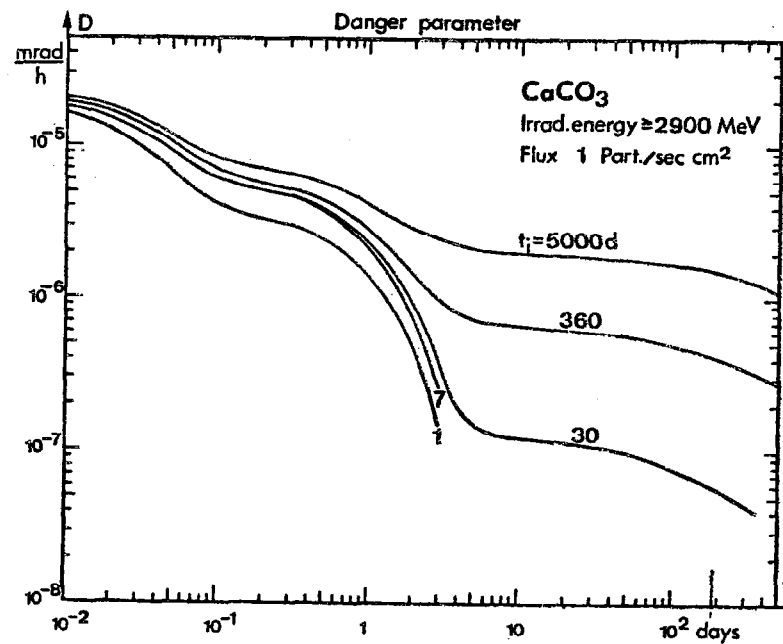
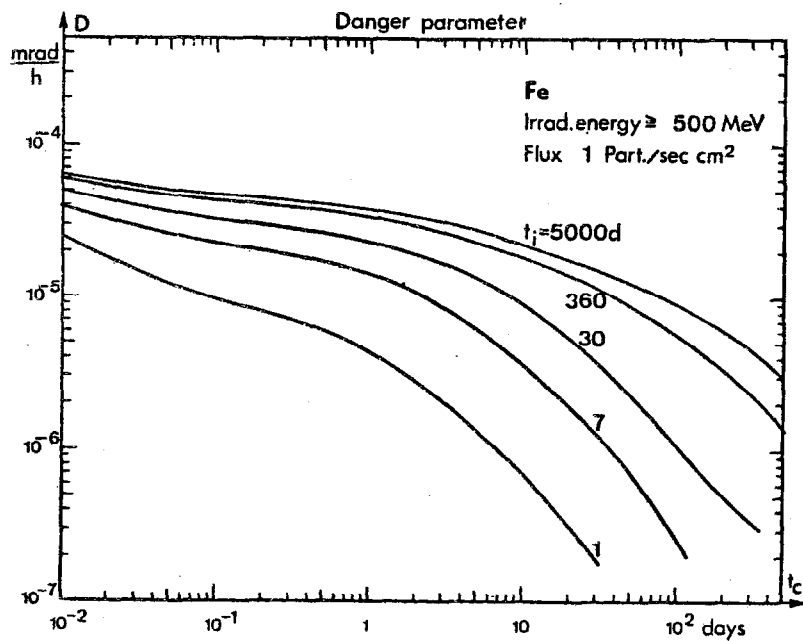
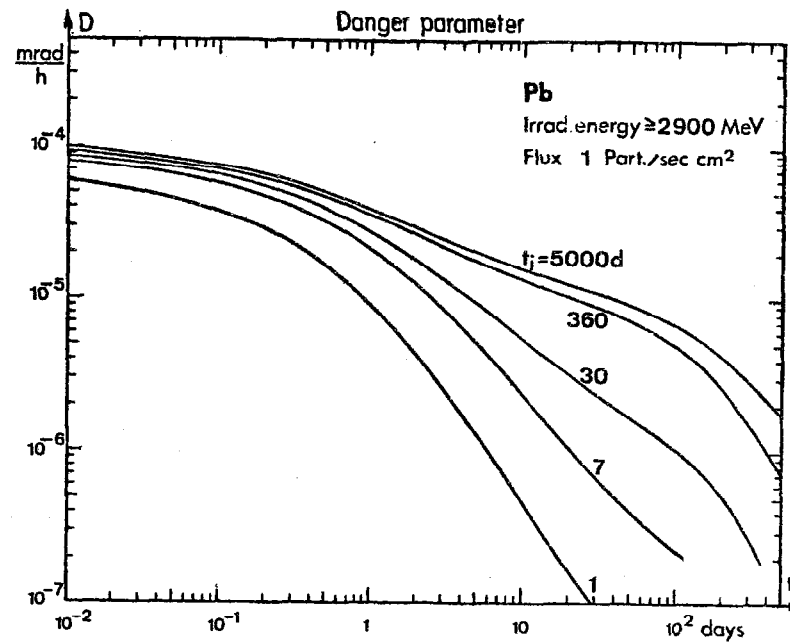
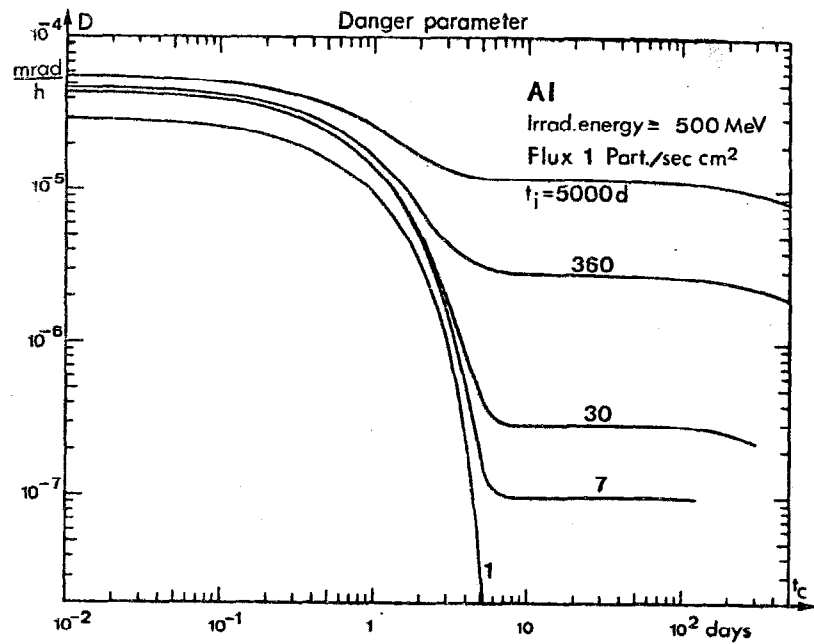


Fig. 3. "Danger parameter" for various materials used in accelerator construction. From Ref. 1

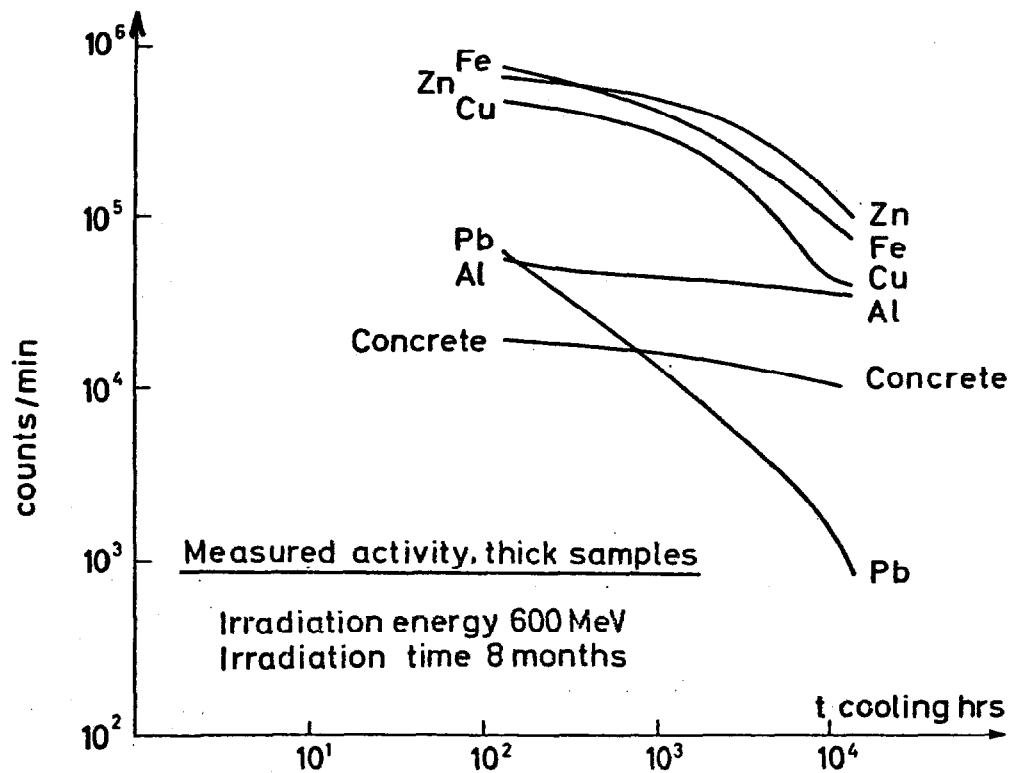
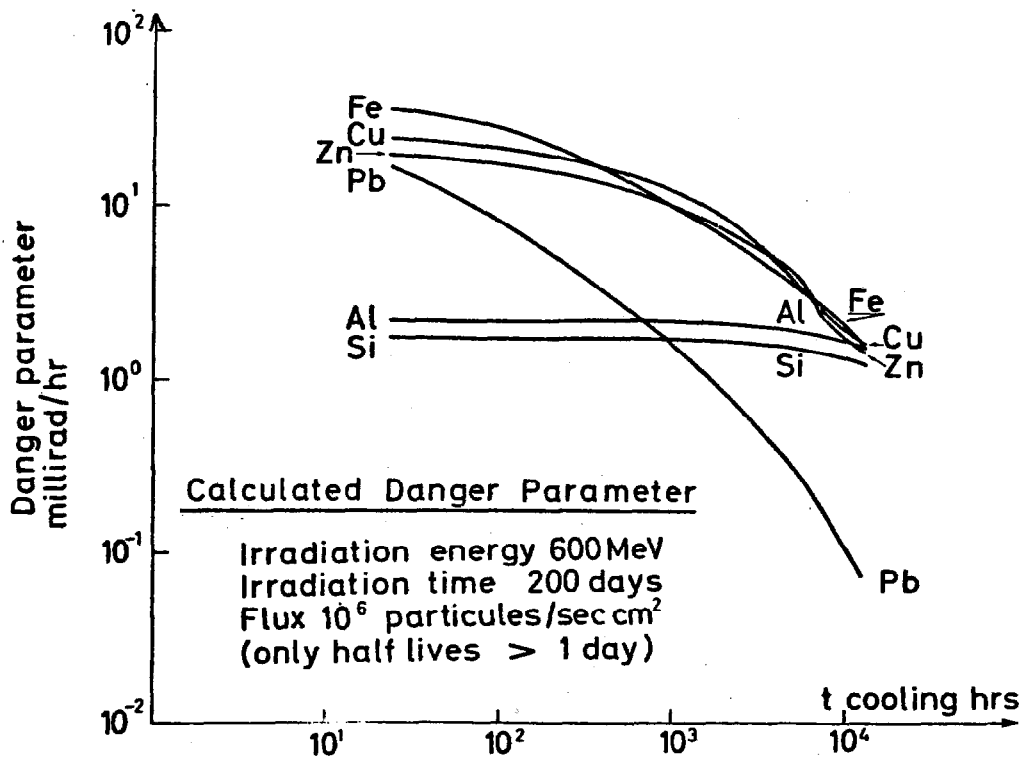


Fig. 4 Measured and calculated cooling curves for several different materials. From T. W. Armstrong, et al., ORNL-TM-2498.

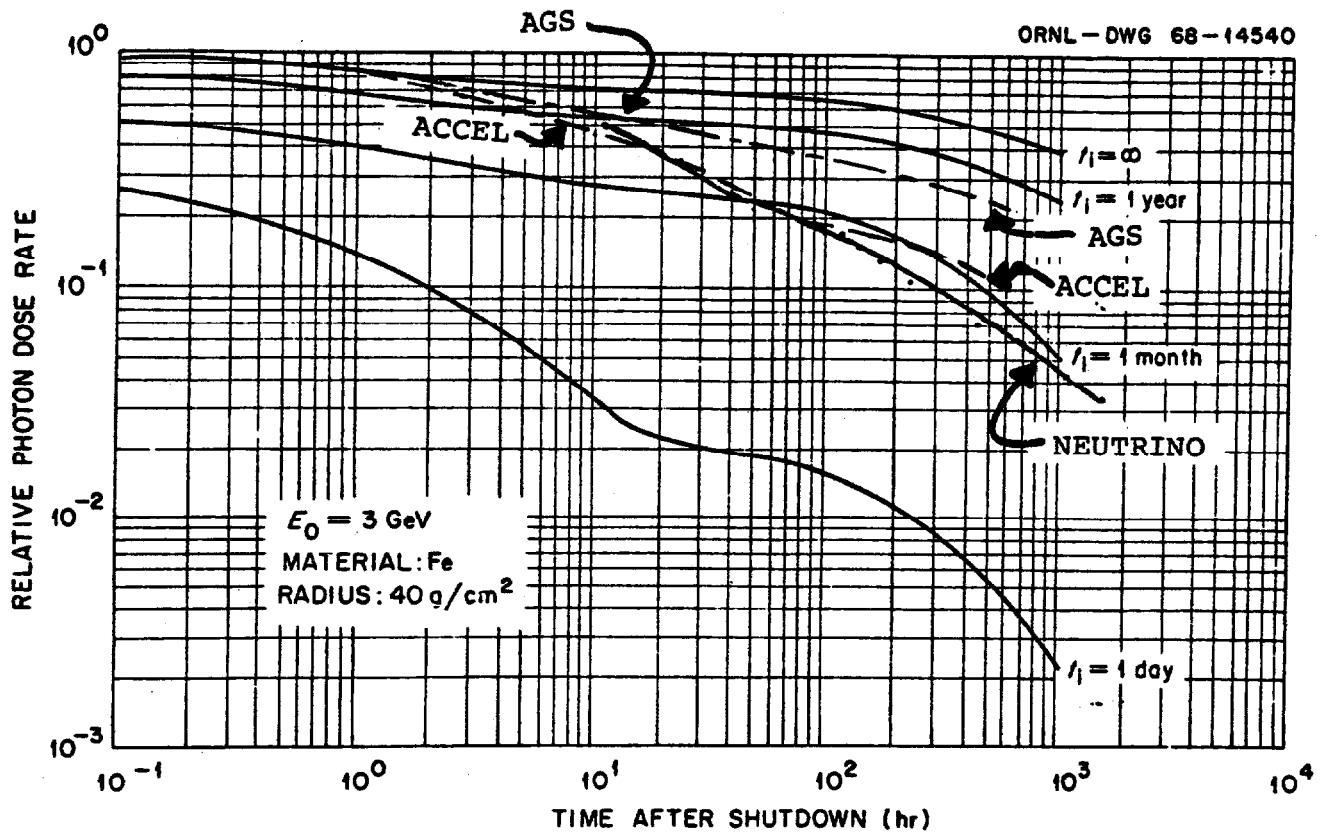


Fig. 5. Calculated cooling curves for various irradiation times for iron struck by high energy protons. (From T. W. Armstrong, et al., ORNL-TM-2498). The curve labeled "accel" is the measured average cooling curve for the Fermilab main ring after three years of operation. The curve labeled "neutrino" is for a neutrino target train after eight months of use. The curve labeled "AGS" is for an extraction splitter in use for many years at the BNL AGS.

Peter J. Gollon
Fermi National Accelerator Laboratory†
Batavia, Illinois 60510

Introduction

At all accelerators with energies greater than some tens of MeV, induced radioactivity results whenever beams interact with accelerator or beam transport components. Typically these interactions occur at injection and extraction points and beam splitting stations. Losses at these points are not desirable, and great efforts are often required to reduce them. Beam losses also occur at collimators, scrapers, target areas and beam dumps; these losses are deliberate and cannot be reduced. Consequently, these are usually the most radioactive areas of the accelerator, and work near them is the largest source of radiation exposure at all laboratories. It is therefore necessary to be able to anticipate the magnitude of the problems involved in such work, in order to minimize those problems in the design of a new facility.

While these loss points are common to all accelerators, the magnitude of the resulting problems depends on many factors unique to each accelerator: the type of particle accelerated, the particle energy, and the geometry and composition of the items being struck. These considerations will be dealt with in turn. What follows is a general introduction for those not actively involved in this area. The literature should be consulted for details.¹

Mechanisms of Activation

Proton Accelerators

The extranuclear hadron cascade process, which has been discussed in previous lectures, produces the major fraction of the induced radioactivity at proton accelerators. Each high energy particle which interacts with a nucleus may be absorbed and/or many knock some nucleons out of the struck nucleus. Additional high energy particles may also be created in the collision. If the resulting nucleus is highly excited, it will de-excite by "boiling off" so-called "evaporation neutrons." The entire nuclear reaction is called a "star" because of the many secondary particles radiating from it.

The resulting nucleus may be stable or radioactive. The cross section for producing a particular nuclide depends on the target nucleus and on the type and energy of the incident particle. These cross sections are best determined from experimental data; if such data is lacking, an empirical formula of Rudstam gives a good approximation to cross sections which vary over several orders of magnitude.²

The particles in the cascade continue to propagate and decay or interact until their energy drops below the threshold for nuclear reactions; this is usually between 10 and 50 MeV. However, for some nuclides, neutron capture is an exoergic reaction which has a large cross section for thermal neutrons. (The radioactivation of concrete occurs principally by thermal neutron capture of ²³Na to produce 15-hour ²⁴Na.)

The excellent book by Barbier contains information on many cross sections which are relevant to radioactivation, and describes how to calculate induced activity levels from such data. Some details of these calculations will be discussed later. First we will discuss some simple rules of thumb which can be used for most "back of the envelope" calculations.

† Operated by Universities Research Association, Inc. under contract with E.R.D.A.

Rule 1: The dose rate \dot{D} (R/hr) at a distance r (meters) from a "point source" of gamma rays is given in terms of the source strength S (Curies) and the photon energy E_γ (MeV), by³

$$\dot{D} \equiv \frac{K_\gamma S}{r^2} \approx \frac{1 E_\gamma S}{2.2 r^2}$$

Rule 2: In many common materials, about 50% of the nuclear interactions produce a radionuclide with a half life longer than a few minutes. About half of these have half lives greater than a day.⁴

Using these rules, we can calculate the dose rate near a target a tenth of an interaction length long. (A much longer target would require a large correction for secondary interactions.) Assume a beam of 10^{11} protons/second has struck the target for several months --long enough for many of the radionuclides produced to reach their saturation levels. Of the 10^{11} p/s incident, one tenth interact, and half of these interactions yield radionuclides of interest. The resulting decay rate is 5×10^9 /s, or 135 mCi. (1 Curie $\equiv 3.7 \times 10^{10}$ disintegrations/second.) Assuming each decay produces a 1 MeV photon, the dose rate half a meter away shortly after beam turnoff is

$$\dot{D} = \frac{(1 \text{ MeV}) \times (0.135 \text{ Ci})}{2.2 \times (0.5\text{m})^2} = 0.245 \text{ R/hr} = 245 \text{ mR/hr}$$

This activity will decay with time in a way which this data cannot predict, but which may be predicted reasonably well by a statistical model of Sullivan and Overton, given below.⁵

Rule 3: For most common shielding materials, the dose rate due to a constant irradiation is given by

$$\dot{D} = b \phi \log \left(\frac{t_i + t_c}{t_c} \right)$$

Here ϕ is the incident flux, b is a material and geometry-dependent constant, and t_i and t_c are the irradiation and cooling times. This is valid for those materials which yield many radionuclides upon irradiation, and for $t_c > 12$ min, $(t_i + t_c) < 500$ days.¹ The constant b may be determined using Rule 2 or experimentally.

Another useful rule relates the total number of stars produced by a single proton in the entire cascade to the incident proton (or hadron) energy:

Rule 4: In a cascade, a proton produces four stars for each GeV of kinetic energy.⁶

Thus a beam of 10^{12} 400 GeV p/s ($=0.16 \mu\text{A}$, or 64 kW) produces a total of $4 \times 400 \times 10^{12} = 1.6 \times 10^{15}$ stars/s in its beam dump. If 25% of the stars yield a radionuclide with a half life greater than a day, then the total amount of moderately long-lived radioactivity in the dump is

$$\frac{(0.25 \text{ dis/star}) (1.6 \times 10^{15} \text{ stars/s})}{3.7 \times 10^{10} \text{ dis s}^{-1} \text{ Ci}^{-1}} = 10 \text{ kCi.}$$

Electron Accelerators

The electron-photon shower, the process whereby high energy electrons interact in bulk matter, is conceptually similar to the hadron shower just described. The principal differences lie in the type of particles which propagate, and in the interactions which produce them. When the initiating electron or photon has an energy greater than several GeV, the predominant interactions are:⁷

*This was a lecture at International School of Radiation Damage and Protection, "Eftore Majorana" Center, Erice, Sept. 1975.

1. *Bremsstrahlung*, in which an e^\pm radiates a photon in the electric field of a nucleus; and
2. *Pair Production*, in which a photon materializes into an electron-positron pair in the electric field of a nucleus.

At lower energies—some tens to a hundred MeV, depending on the material—the following processes for reducing the electron or photon energies become important:

3. *Electron-Electron Collisions* (ionization), in which an incident electron elastically scatters from an atomic electron, resulting in two lower energy electrons;
4. *Compton Scattering*, in which photons elastically scatter from atomic electrons, transferring some of their energy to the electrons.

The longitudinal development of the shower is characterized by a quantity known as the "radiation length," X_0 . It is the distance in which the average energy of an electron or photon is reduced by a factor of e . Since the bremsstrahlung and pair production cross sections are proportional to Z^2 , X_0 is approximately proportional to AZ^{-2} . Radiation lengths for common materials range from 65 gm/cm² for beryllium to 6.5 gm/cm² for lead.

The number of electrons and photons in the shower increases exponentially with depth (as e^{x/X_0}), with additional electrons and photons being produced by pair production and bremsstrahlung. This continues until the average particle energy is below the "critical energy" for that material; at this point ionization and Compton scattering play a dominant role in removing energy from the shower, and particle multiplication ceases. Because of random variations in each interaction, the cascade dies off only slowly when the mean particle energy reaches the critical energy. The electron shower is therefore characterized by a rapid exponential rise to a maximum, followed by a slower fall.

The shower consists of equal numbers of positrons, electrons, and photons, but only the photons play a significant role in producing nuclear reactions. Most significant are the (γ, n) , $(\gamma, 2n)$, (γ, p) , (γ, pn) and (γ, α) photonuclear reactions.

Each interaction of a high energy photon reduces its energy by a factor of two, on the average, while the average number of photons in each generation doubles. Considering photons of all generations in a shower initiated by an electron of energy E_0 , the total track length $g(E)dE$ is the total distance travelled in the shower by all photons which have energies between E and $E+dE$. It is given by⁸

$$g(E)dE = 0.57 \frac{E_0}{E^2} X_0 dE \text{ (gm/cm}^2\text{)}$$

The track length is multiplied by the number of target nuclei per gram and by the reaction cross section to obtain the number of photonuclear reactions initiated by photons of energy E . We then integrate over all possible photon energies to obtain the number of photonuclear reactions in the cascade:⁹

$$Y = 0.57 \frac{E_0 X_0 N_0}{A} \int_0^{E_0} \frac{\sigma(E)}{E^2} dE$$

Two factors combine to allow an approximation to the integral. First, the photonuclear cross sections are dominated by the "giant resonance" phenomenon which occurs between 20 and 50 MeV; other processes occur less frequently. In addition, the photon spectrum is a sharply falling function of energy. The denominator (E^2) may be taken to be equal to its value (E_m^2) at the cross section maximum, and moved outside the integral:

$$Y = 0.57 \frac{E_0 X_0 N_0}{A E_m^2} \int_0^{E_0} \sigma(E) dE$$

Barbier¹ presents curves of integrated cross sections as a function of target mass for the five photonuclear reactions of interest, in which he has combined all the factors in the last equation except for the incident electron energy. To find the number of reactions produced in a shower due to an incident electron of energy E_0 , one multiplies the giant resonance yield (read from the appropriate graph) by E_0 .

As an example, we calculate the total activity created in an iron dump (assumed to be 100% ^{56}Fe) by a 1 μA , 20 GeV electron beam (20 kW of power). The most significant reaction is $^{56}\text{Fe}(\gamma, pn) ^{54}\text{Mn}$. The yield for this reaction is 3×10^{-6} per MeV. The incident beam is

$$\frac{10^{-6} \text{ Coul/s} \times 2 \times 10^4 \text{ MeV}}{1.6 \times 10^{-19} \text{ Coul}} = 1.25 \times 10^{17} \text{ MeV/s}$$

The reaction rate is then

$$Y = 1.25 \times 10^{17} \text{ MeV/s} \times 3 \times 10^{-6} / \text{MeV} = 3.8 \times 10^{11} \text{ s}^{-1}$$

When the 300-day half life ^{54}Mn has been saturated, this will be a total activity of 10 Ci. This is about 1/300 of the activity produced in an iron dump by a proton beam of the same power.

Usually several photonuclear reactions will contribute significantly to the activation of a target material. The residual radiation level may then be obtained by summing the yields for the various reactions, weighted appropriately to allow for the buildup and decay of each radionuclide. Figure 1 shows such decay curves for various common materials after an infinitely long electron irradiation; the large differences in residual dose rate indicate the importance of the proper choice of material.

Relation Between Hadron and Electron Showers

While hadron and electron showers were discussed separately, they are in fact physically connected. In hadron-initiated interactions, about one third of the pions produced are uncharged. These promptly decay into two high-energy photons, which start electron showers. At 400 GeV, about half of the incident proton beam energy is thus dissipated in the form of electron showers. However, electron showers are much less effective than hadron showers, per MeV of energy, at producing radioactivity, so that this effect may be ignored in hadron cascades.

Conversely, the photonuclear reactions which occur in electron showers liberate nucleons from the struck nuclei. However, since most of these reactions occur near 50 MeV, the escaping nucleons do not have much energy. They are therefore not likely to interact further except by neutron capture, and whether this yields a significant amount of radioactivity depends on the specific materials involved.

Calculational Techniques: Comparison With Experiment

In order to provide more accurate, and thus more useful information concerning dose rates due to activation, we must have detailed information in the following areas:

cascade source term: the spatial distribution and spectra of the particles in the hadron or electron shower in the "target" of interest;

nuclear reaction data: reaction cross sections for transforming various nuclei in the "target" into other, radioactive nuclei;

radiological data: nuclear lifetimes, decay schemes, transport of β 's and γ 's out of the activated object (i.e., self-shielding) and flux-to-dose conversion factors.

There are several calculational approaches. Alsmiller and co-workers at Oak Ridge use the most involved technique: they Monte Carlo the cascades, including the intra-nuclear details of each reaction, and

then carefully calculate the transport of the decay γ -rays out of the material.¹⁰ They are then able to predict the spatial distribution of each spallation product. This method is powerful but cumbersome, and is not used routinely elsewhere.

A different approach is used by Barbier¹. He separates the problem into two parts: the user is given the task of determining the flux of activating particles (hadrons or photons), while Barbier provides information on residual dose rate per unit activating flux. Barbier derives his induced spallation cross sections from an empirical formula of Rudstam² (this formula was derived for proton-induced reactions, but is used to describe all hadron-induced reactions), and from his own smooth fits to measured photonuclear cross sections. Experimental values of nuclear lifetimes and decay characteristics were entered into these calculations. Transport of β and γ rays out of the material and conversion to dose rate was done in an approximate analytic way. The results may be presented in terms of what Barbier calls the "danger parameter." This is the dose rate in a cavity inside an infinite volume of radioactive substance of uniformly distributed activity produced by unit hadron flux (1 particle/cm²-sec). Curves of danger parameters for different materials are shown in Figure 2 which are similar to conventional "cooling curves." The danger parameter is a function of irradiation and cooling time because isotopes with different lifetimes saturate and decay differently with time. These calculations yield results comparable to those of the Oak Ridge group—compare Figures 2 and 4.

We can use one of these curves to determine the dose rate in a real situation involving a thick source by using the following relation:

$$\dot{D} = \frac{\Omega}{4\pi} \cdot \phi \cdot d = \frac{\Omega}{4\pi} \cdot S \cdot \omega$$

The dose rate at any point (\dot{D}) is obtained by multiplying the danger parameter (\dot{D}) by the fractional solid angle (Ω) the source subtends when seen from the point of interest, and by the activating flux (ϕ) at the surface of the object.¹¹ (The activity several γ absorption lengths into the body does not contribute much to the external dose rate because of self-shielding by the activated object.) An alternate representation involves the hadron star density S in the activated material and a different parameter, ω . The flux and star density are of course related: $\phi = \lambda S/\rho$; λ being the interaction length and ρ the density of the material.

It is possible to obtain the hadron flux at the surface of the object from a Monte-Carlo calculation run for that purpose, or from a collection of "standard" cases.^{12,13} If this is done, one must be careful because many Monte Carlo programs have a low-energy cutoff, below which they cease to follow particles. Since this cutoff may be higher than the thresholds of many activation reactions, use of the "flux" or "star density" predicted by the Monte Carlo calculation will give an erroneously low value for the activation. Correction for this effect may be made if the ratio of the true flux to the "Monte Carlo flux" is known. This ratio is material-dependent, and to the extent that the spectrum has not reached an equilibrium shape, it is position-dependent as well.

For the 300 MeV/c cutoff used by Van Ginneken, the proportionality constant for iron, $\omega(t_i, t_c)$, is

$$\omega(\infty, 0) = 9 \times 10^{-6} \text{ rad hr}^{-1} (\text{star cm}^{-3} \text{s}^{-1}), \text{ or}$$

$$\omega(30d, 1d) = 2.5 \times 10^{-6} \text{ rad hr}^{-1} (\text{star cm}^{-3} \text{s}^{-1})$$

Curves of the danger parameter (Fig. 2) may be used to calculate the residual activity of various materials for different irradiation and cooling times. They may also be used for irradiation times other than the standard ones presented in the figures, as follows:

The dose rate after an irradiation time t_i and a cooling time t_c is

$$\dot{D}(t_i, t_c) = \sum_{\mu} A_{\mu} \{1 - \exp(-t_i/\tau_{\mu})\} \exp(-t_c/\tau_{\mu})$$

The summation μ is over all relevant radionuclides with lifetimes τ_{μ} ; A_{μ} are appropriate constants. Rearranging the factors,

$$\dot{D}(t_i, t_c) = \sum_{\mu} A_{\mu} \{ \exp(-t_c/\tau_{\mu}) - \exp(-[t_i+t_c]/\tau_{\mu}) \} = \dot{D}(\infty, t_i) - \dot{D}(\infty, t_i+t_c)$$

Thus the dose rate sought is the difference between the dose rates for the case of an infinite irradiation time and two hypothetical cooling times: one equal to the actual irradiation time, the other equal to the actual irradiation plus cooling times. This formula is exact, and does not depend on the validity of any model of the radioactivation process.

It is far easier to make predictions of induced radioactivity than it is to verify those predictions, thus experimental data is hard to come by. Figure 3 shows measurements and calculations made by Barbier and Cooper at CERN.¹⁴ The average difference between prediction and measurement is about a factor of two. Other comparisons show similar agreement, especially for relatively short irradiation times.^{13,15} When known cross sections and thin targets are used, the agreement is better.¹⁶

Applications

Life is not really as simple as one might believe from the previous sections. First, calculations by different authors disagree with each other, often by factors of two. Second, real life sometimes does not reproduce any author's calculation. (Fortunately, things seem to cool off faster in real life than they do in calculations.) Figure 4 shows a calculation from Oak Ridge, to which has been added the decay curves of a number of accelerator components made mostly of iron. The curve labelled "accel" is based on the measured cooling of the average dose rate around our 6-km circumference main accelerator.¹⁷ It has been operating for 3 years with essentially constant losses, thus the curve ought to be comparable to the one labelled "one year"; but it falls about a factor of 3 below it for long cooling times.

The curve labelled "neutrino" represents the decay of an area near the target of our dichromatic (narrow band) neutrino target train after a run of 8 months.¹⁸ The beam intensity varied by a factor of about two over this period. Again, the components cooled much faster than one would predict.

Finally, the curve marked "AGS" represents the dose rate near the Brookhaven AGS slow external beam splitter.¹⁹ This unit has been operating for many years, and its decay agrees reasonably well with the predictions for long irradiations. The most obvious explanation for the disagreement of observations and calculations is that possibly a lot less long-lived activity than is expected is actually being produced. There is no data to substantiate or refute this conjecture, however.

As can be seen from the various graphs of the danger parameter, different materials vary widely in their relative hazards due to activation. Aluminum is preferred to iron because of its lesser activation—the only major long-lived activity produced from aluminum is ²²Na. For shielding purposes, CaCO₃—the principal constituent of marble—is excellent for the same reason; in this case the cross section for ²²Na production from calcium is even lower. Elements above calcium, however, are capable of readily producing long-lived activity.²⁰

Sodium, on the other hand, is notorious for causing problems because of its high thermal neutron capture cross sections, producing ^{24}Na . The effects of even small amounts of sodium in concrete have been studied extensively both theoretically and experimentally.²¹ Briefly, concrete containing one percent of sodium by weight produces enough ^{24}Na activity to approximately double the radiation level in the machine enclosure the first day after machine turn-off. Since the major source of sodium in concrete is the aggregate, a proper choice of aggregate, such as limestone, can eliminate this problem. We have recently seen evidence for the copious production of $2.6 \text{ hr } ^{56}\text{Mn}$ by thermal neutron capture on traces of ^{55}Mn in iron and concrete. The neutron spectrum emanating from a thick 1 m radius iron shield was particularly rich in intermediate energy and thermal neutrons;²² additional thermalization occurred in the concrete. Traces of boron added to the concrete in the area would capture most of the neutrons and alleviate the problem.

The question of radioactivation of air in target and accelerator enclosures has been studied at some length.²³ It has been our experience, and that of others, that because of the short half-lives involved (20 min ^{11}C is the longest apart from tritium) there is no internal exposure hazard. There is an external exposure hazard, but that is smaller than, and no different from the hazard due to radioactivated accelerator components in the same area.

References

1. M. Barbier, Induced Radioactivity, North Holland (1969). This is a comprehensive treatise and contains references to other works not cited below.
2. R. G. Rudstam, Z. Naturforsch. 21a 7 (1966).
3. More exact values of k_γ may be found in Ref. 1, Appendix A; values of a proportional quantity may be found in Radiological Health Handbook, p. 131, U.S. Dept. of HEW (1970).

4. A. H. Sullivan, Health Physics 23 253 (1972). See Also Ref. 1, pp 19-27.
5. A. H. Sullivan and T. R. Overton, Health Physics 11 1101 (1965).
6. This is true for stars produced by particles above a 15 MeV cutoff in iron. There are about half as many stars produced by particles above a 100 MeV cutoff. R. T. Santoro and T. A. Gabriel, ORNL-TM-3335 (1971).
7. R. B. Leighton, Principles of Modern Physics p. 690 McGraw-Hill (1959).
8. B. Rossi, High Energy Particles, p. 271, Prentice Hall (1952).
9. Ref. 1, p. 217.
10. See, for example, T. W. Armstrong, et al., Nucl. Sci. Eng. 49, 82 (1973); T. W. Armstrong and R. G. Alsmiller, Jr., ORNL-TM-2498 (1969).
11. Ref. 1, p. 77.
12. A. Van Ginneken and M. Awschalom, High Energy Particle Interactions in Large Targets, Fermilab ('75).
13. M. Hofert, et al., CERN DI/HP/185 (1975).
14. M. Barbier and A. Cooper, CERN 65-34 (1965).
15. M. Hofert and A. Bonifas CERN HP-75-148 (Internal Report) (1975).
16. K. S. Toth, et al., Nucl. Inst. and Meth., 42, 128 (1965).
17. H. Casebolt and J. McCrary, private communication.
18. S. Velen, private communication.
19. R. Casey, private communication.
20. Ref. 1, p. 37.
21. D. Nachtigall and S. Charalambus, CERN 66-28 (1966); W. S. Gilbert, et al., UCRL-19368 (1969); P. J. Collon, et al., NAL-TM-250 (1970); T. W. Armstrong and J. Barish, ORNL-TM-2630 (1969).
22. R. G. Alsmiller, Jr., and J. Barish, Particle Accel 5 155 (1973).
23. M. Hofert, Proc. Sec. Int'l. Conf. on Accel Dosimetry and Experience, p. 111, Conf-691101 (1969).

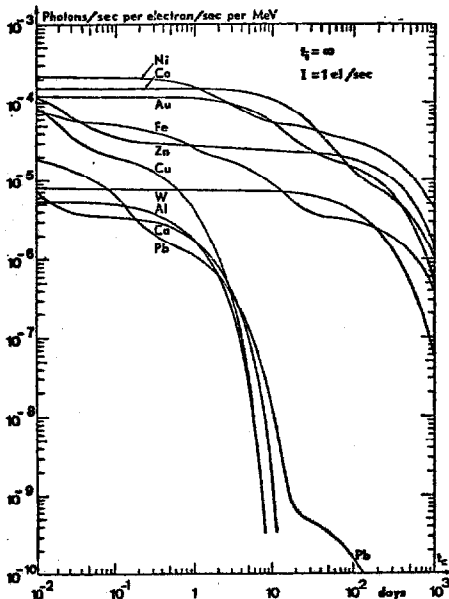


Fig. 1 Total photon emission rate from radioactive nuclei in large targets irradiated by an electron current of 1 electron/second, per MeV incident electron energy. From ref. 1.

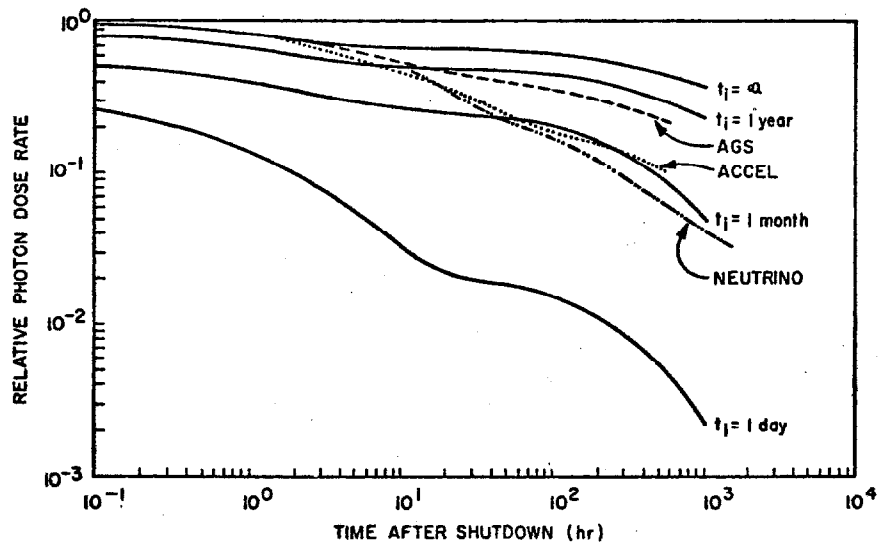


Fig. 4 Calculated cooling curves for various irradiation times for iron struck by high energy protons. (From T. W. Armstrong, et al., ORNL-TM-2498). The curve labeled "accel" is the measured average cooling curve for the Fermilab main ring after three years of operation. The curve labeled "neutrino" is for a neutrino target train after eight months of use. The curve labeled "AGS" is for an extraction splitter in use for many years at the BNL AGS.

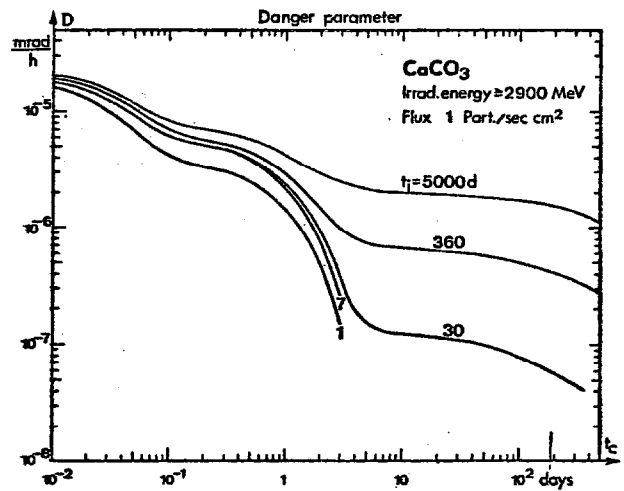
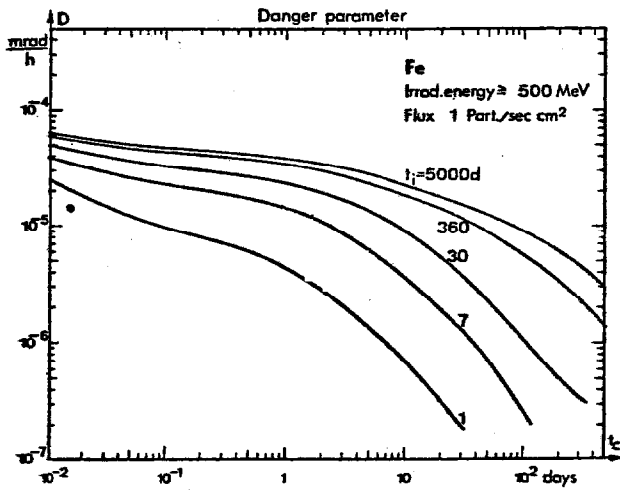
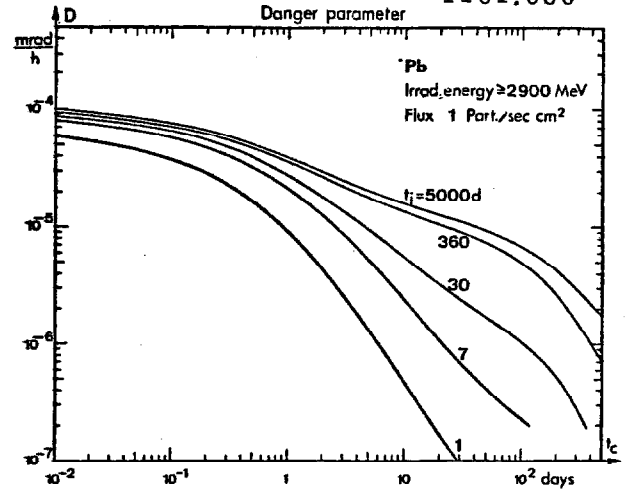
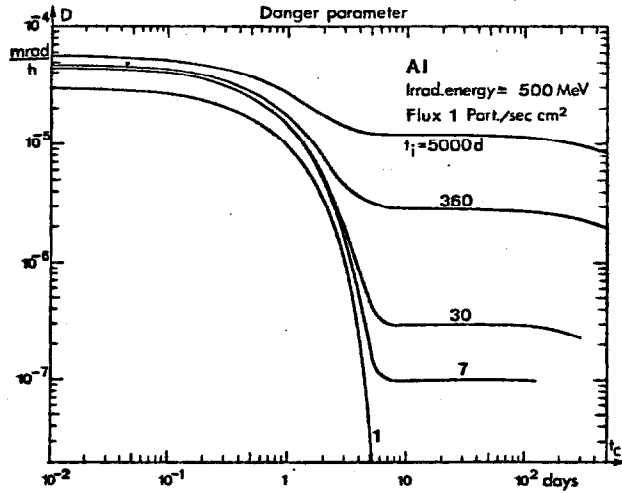


Fig. 2 "Danger parameter" for various materials used in accelerator construction.
From ref. 1.

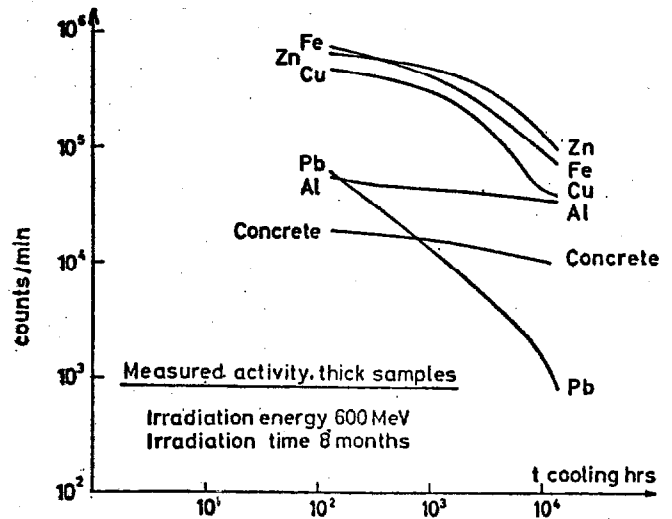
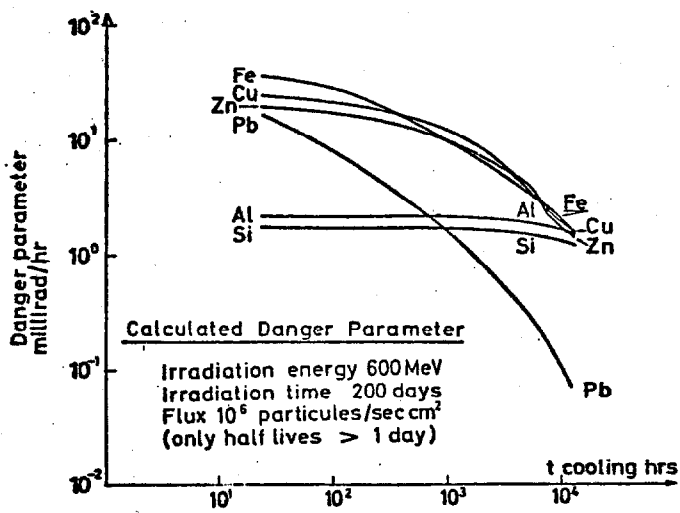


Fig. 3 Measured and Calculated Cooling curves for several different materials.
From ref. 14.